



Inhibited concentration quench effect in upconversion luminescence of $\text{In}_2\text{O}_3:\text{Yb}^{3+}, \text{Er}^{3+}$ inverse opals

Yongsheng Zhu^{a,b}, Yinhua Wang^b, Hairu Xu^b, Xiumei Xu^{b,*}, Jinshu Huang^b, Dongfang Qiu^b, Zhiwen Lu^b, Jiwei Wang^{c,*}

^a State Key Laboratory on Integrated Optoelectronics, College of Electronic Science and Engineering, Jilin University, 2699 Qianjin Street, Changchun 130012, China

^b College of Physics and Electronic Engineering, College of Chemistry and Pharmaceutical Engineering, Nanyang Normal University, Nanyang 473061, China

^c College of Physics, Liaoning University, Shenyang 110036, China

ARTICLE INFO

Keywords:

Upconversion
Photonic crystal
Modification
Concentration quenching

ABSTRACT

The modification of upconversion luminescence (UCL) in $\text{In}_2\text{O}_3:\text{Yb}^{3+}, \text{Er}^{3+}$ inverse opal photonic crystals (IOPCs) was investigated. The spontaneous decay rate (SDR) of $^4\text{S}_{3/2}-^4\text{I}_{15/2}$ in IOPCs was suppressed as high as 2.6 times in contrast to the reference (REF) sample due to the modification of effective refractive index. It is significant to observe that the temperature quenching and concentration quenching in the $\text{In}_2\text{O}_3:\text{Yb}^{3+}, \text{Er}^{3+}$ IOPCs was greatly suppressed due to the thin layer structure and connected air cavity.

1. Introduction

Since the concept of photonic crystals (PCs) was first mentioned by Yablonovitch [1] and John [2] in 1987, these special structures have attracted considerable attention in the fields of near-zero threshold lasers, quantum computer, sensors, light waveguides, photonic crystal fibers, because PCs possess spatial periodicity in their dielectric constant on the length scale of the optical wavelength and behave with respect to electromagnetic waves like atomic crystals do with respect to electrons [3–5]. Among these applications, one which has such interesting physical issue is the modification of the spontaneous emission. Up to now, a number of works have been performed in the field, and some interesting phenomena have been observed such as the observation of the Lamb shift [6], inhibited downconversion concentration quench and local thermal effect [7], and enhanced upconversion (UC) luminescence in IOPCs [8]. The UCL of rare earth (RE) ions is attracting current interests due to its special nonlinear populating mechanism and application potential on the fields of color display, laser, biosensors, bio-imaging and etc. [9–12]. Recently, Yang successfully prepared $\text{NaYF}_4:\text{Yb}^{3+}, \text{Tm}^{3+}/\text{Er}^{3+}$ inverse opal photonic crystals through a novel solvent-thermal Y_2O_3 template method and observe $\text{NaYF}_4:\text{Yb}^{3+}, \text{Tm}^{3+}/\text{Er}^{3+}$ IOPCs showed an observably improved upconversion luminescence ratio in contrast to the reference sample [13]. Wang fabricated $\text{NaGd}(\text{WO}_4)_2:\text{Yb}^{3+}/\text{Tm}^{3+}$ inverse opal photonic crystals (IOPCs) through the polymethylmethacrylate (PMMA) template and detailedly studied the modification of the IOPCs structure on the emission spectra and dynamics of Tm^{3+} ions was systemically [14].

Despite, the work related to the modification of PCs on UCL of embedded RE ions is still rare and further work should be performed to fabricate more RE doped IOPCs and deeply understand its unique physical nature (such as concentration quenching in RE doped UC inverse opal).

In this paper, we present the self-assembly and highly modified upconversion luminescence properties of $\text{Yb}^{3+}, \text{Er}^{3+}$ co-doped In_2O_3 inverse opal. As a very important wide-band-gap n-type semiconductor, In_2O_3 has been extensively studied for various applications, including photocatalysis, liquid-crystal displays, and gas sensors for detection of NO_2 [15–17] and $\text{Yb}^{3+}/\text{Er}^{3+}$ codoped In_2O_3 is an candidate material of the photon energy conversion for solar cell [18]. The refractive index of In_2O_3 is as high as 1.98, thus it is a suitable system to examine the PCs effect on energy transfer. The modification of photonic stop bands (PSBs) on UC emission and spontaneous emission rate in $\text{In}_2\text{O}_3:\text{Yb}^{3+}, \text{Er}^{3+}$ IOPCs was studied detailedly. It is worthy to note that aside from their fascinating optical properties, inverse opal materials are attracting attention because of their inherent structural and physical properties, such as high surface area and three-dimensional (3D) ordered macroporous structure, which makes them desirable for temperature quenching and concentration quenching.

2. Experiments

2.1. Sample preparation

The $\text{In}_2\text{O}_3:\text{xYb}^{3+}, \text{yEr}^{3+}$ ($\text{x} = 15 \text{ mol\%}$ $\text{y} = 0.5, 1, 2, 3, 4, 5, 6 \text{ mol}$

* Corresponding authors.

E-mail addresses: x.m.xu@163.com (X. Xu), jiweiwang6688@yahoo.com (J. Wang).

%) IOPCs were prepared by the sol-gel method with a poly-methylmethacrylate (PMMA) latex sphere template technique. Firstly, monodisperse PMMA nano spheres ($\sim 355, 370, 405$ and 490 nm) were synthesized [19]. Then, the opal templates were self-assembled through the vertical deposition process. The colloid suspension (8% solid content) of PMMA microspheres was dropped onto a quartz glass substrate and placed in a 45°C oven for one day. The PMMA colloidal spheres were slowly self-organized into highly ordered colloidal arrays on the glass substrate, driven by capillary force of the liquid in the evaporating process. In the preparation of the $\text{In}_2\text{O}_3:\text{Yb}^{3+}, \text{Er}^{3+}$ precursor sol, stoichiometric amounts of $\text{In}(\text{NO}_3)_3 \cdot 4.5\text{H}_2\text{O}$, $\text{Yb}(\text{NO}_3)_3 \cdot 6\text{H}_2\text{O}$, $\text{Er}(\text{NO}_3)_3 \cdot 6\text{H}_2\text{O}$ were dissolved in 10 ml water solution. Then, 500 mg citric acid contained in the mixed solution was used as the chelating agent. The mixture was stirred for 3 h, forming a transparent solution. The prepared precursor solutions were used to infiltrate into the voids of the opal templates. After infiltration, the resulting products were dried in air at room temperature for one day. Annealing was carried out with slowly elevated temperature ($40^\circ\text{C}/\text{h}$) up to 500°C for 3 h. Samples prepared by opal templates constructed with PMMA microspheres $\sim 355, 370, 405$ and 490 nm in diameter were denoted as samples PC1 to PC4, respectively. For comparison, the reference (REF) samples were prepared, firstly, the IOPCs (PC1-PC4) were scraped from the glass substrates, then grind the IOPCs in the mortar for 5 min to destroy the regular three-dimensional order structure.

2.2. Characterization and measurements

The morphology of the samples was measured with a JEOL JSM-7500 field emission scanning electron microscope (FE-SEM) at an accelerating voltage of 15 kV. The phase structure of the samples were

characterized by X-ray diffractometer, using a monochromatized Cu target radiation resource ($\lambda = 1.54 \text{ \AA}$). Transmittance spectra were measured with a Shimadzu UV-3101PC scanning spectrophotometer with a range of $200\text{--}1100$ nm. A continuous 980-nm diode laser was used to pump the samples in order to investigate the steady-state spectra. The luminescent dynamics of Er^{3+} ions were investigated by a laser-system consisting of a Nd:YAG pumping laser (1064 nm), a third-order Harmonic-Generator (355 nm) and a tunable optical parameter oscillator (OPO, Continuum Precision II 8000). The laser has pulse duration of 10 ns, repetition frequency of 10 Hz and line width of $4\text{--}7 \text{ cm}^{-1}$.

3. Results and discussion

Fig. 1(a) shows that long range PMMA opal template is formed, and the diameter of the PMMA spheres is 370 nm. The PC2 sample yields a long-range ordered hexagonal arrangement of inverse opal with the center-to-center distance of ~ 260 nm between the macropores on the (111) planes (as shown in Fig. 1(b)), which is about 30% smaller than the original size of the PMMA template due to the shrinkage of spheres during calcination. An enlarged TEM image (see Fig. 1(c)) shows that the wall thickness of IOPCs is about ~ 20 nm, which consists of a large amount of small nanoparticles. Fig. 1(d) shows the XRD patterns of the $\text{In}_2\text{O}_3:\text{Yb}^{3+}, \text{Er}^{3+}$ IOPCs and REF sample in contrast to the standard card. It can be seen that all of the samples are exactly in agreement with the corresponding standard cards, JCPDS 65-3170 for cubic In_2O_3 crystal. No impurity peaks appear, implying that the samples are both $\text{In}_2\text{O}_3:\text{Yb}^{3+}, \text{Er}^{3+}$ in pure cubic phase. Note that except for the center-to-center distances, the samples PC1, PC3, and PC4 are similar to PC2.

The transmittance spectra of the IOPCs were measured at the

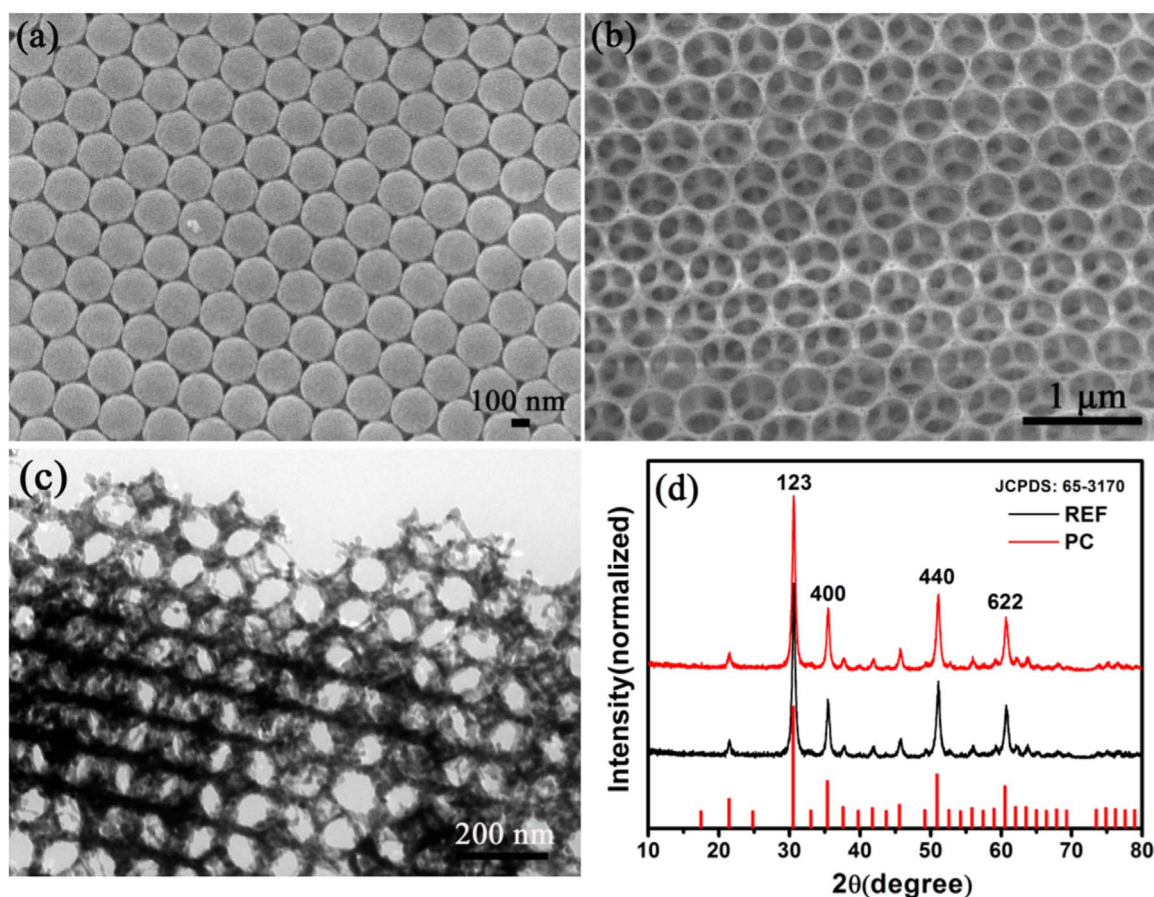


Fig. 1. (a) SEM image of the PMMA opal template sample; (b) SEM image of the $\text{In}_2\text{O}_3:\text{Yb}^{3+}, \text{Er}^{3+}$ inverse opal sample; (c) TEM image of the $\text{In}_2\text{O}_3:\text{Yb}^{3+}, \text{Er}^{3+}$ inverse opal sample; (d) the XRD patterns of $\text{In}_2\text{O}_3:\text{Yb}^{3+}, \text{Er}^{3+}$ IOPCs and REF samples.

Download English Version:

<https://daneshyari.com/en/article/7840602>

Download Persian Version:

<https://daneshyari.com/article/7840602>

[Daneshyari.com](https://daneshyari.com)